A Geometric Sequence that Accurately Describes Allowed Multiple Conductance Levels of Ion Channels: The "Three-Halves (3/2) Rule"

John R. Pollard, Nelson Arispe, Eduardo Rojas, and Harvey B. Pollard
Laboratory of Cell Biology and Genetics, National Institute of Diabetes, Digestive and Kidney Diseases, National Institutes of Health, Bethesda, Maryland 20892 USA

ABSTRACT Ion channels can express multiple conductance levels that are not integer multiples of some unitary conductance, and that interconvert among one another. We report here that for 26 different types of multiple conductance channels, all allowed conductance levels can be calculated accurately using the geometric sequence $g_n = g_o(3/2)^n$, where g_n is a conductance level and n is an integer ≥ 0. We refer to this relationship as the "3/2 Rule," because the value of any term in the sequence of conductances (g_n) can be calculated as 3/2 times the value of the preceeding term (g_{n-1}). The experimentally determined average value for "3/2" is 1.491 ± 0.095 (sample size = 37, average ± SD). We also verify the choice of a 3/2 ratio on the basis of error analysis over the range of ratio values between 1.1 and 2.0. In an independent analysis using Marquardt's aligorithm, we further verified the 3/2 ratio and the assignment of specific conductances to specific terms in the geometric sequence. Thus, irrespective of the open time probability, the allowed conductance levels of these channels can be described accurately to within ~6%. We anticipate that the "3/2 Rule" will simplify description of multiple conductance channels in a wide variety of biological systems and provide an organizing principle for channel heterogeneity and differential effects of channel blockers.

INTRODUCTION

Ion channels are routinely described in terms of their conductance as obtained from the slope of a linear portion of a current-voltage relationship (I-V curve), and in many cases the conductance is sufficient to identify the channel (Edwards, 1982; Hille, 1984). However, there are several examples of ion channels that, at a fixed voltage, express multiple levels of conductance. These levels appear to interconvert amongst one another, and are not integer multiples of some unitary level of conductance (Fox, 1987; Meves and Nagy, 1989). The best known examples include the small molecule, alamethicin (Baumann and Meuller, 1974; Gordon and Haydon, 1972; Hanke and Boheim, 1980), and other antibiotics (for review, see Latorre and Alvarez, 1981). Conventional membrane resident channels with multiple conductance levels include the "double barrelled" anion channel from Torpedo (Miller, 1982; Bauer et al., 1991); cation channels regulated by excitatory amino acids such as *N*-methyl-D-aspartic acid (NMDA), glutamate, kainate, and quisqualate (Cull-Candy and Usowicz, 1987; Jahr and Stevens, 1987); glycine and gamma-amino-butyric acid (GABA)-gated channels from spinal cord (Smith et al., 1989); acetylcholine receptor channels from muscle (Hamill and Sakmann, 1981); the recombinant nucleotide binding fold anion channel from the CFTR (Arispe et al., 1992a); gap junction channels (Spray and Bennett, 1985; Young et al., 1987); ryanodine-sensitive calcium channels (Liu et al., 1989), and dihydropyridine (DHP)-sensitive calcium channels (Ma and Coronado, 1988) in muscle; and others to be described below. It is not uncommon to find at least 5 or 6 conductance levels in many of these channel systems.

There are two alternative explanations for multiple conductance channels. The first considers that the cross sectional area of a single channel can vary (e.g., Stein, 1986). The other proposes the coexistence of multiple channels of identical conductance which open in concert. According to the latter model, the different conductances should be exact integer multiples of a minimum conductance, as noted for Torpedo anion channels studied in natural abundance (Miller, 1982) or as recombinant molecules (Bauer et al., 1991). Analogous biophysical arguments have been made for other systems, including "double-barrelled" chloride channels from rabbit cortical collecting duct (Sansom et al., 1990), "triple-barrelled" potassium channels from guinea pig heart cells (Matsuda et al., 1989), and even a "16-barrel" channel from a molluscan neuron (Geletyuk and Kazachenko, 1985). However, we have learned that most systems do not necessarily express conductance levels as integral multiples of one minimal conductance, although the data are frequently interpreted in this manner. In addition it is difficult to fit the observed frequency of simultaneous openings to the expected binomial distribution.

Our alternative approach, as described below, was to examine the set of observed values of conductance for each channel, in sequence, and to search for any regular relationship among the members of each set. We found that for all the channel systems examined, the conductance values, g_n, expressed by the channel could be accurately described by recourse to the following geometric sequence:

$$g_n = g_o\{3/2\}^n,$$

where g_o is the minimum conductance, and the integer n (≥ 0)

Received for publication 14 October 1993 and in final form 13 April 1994.
Address reprint requests to Harvey B. Pollard, Laboratory of Cell Biology & Genetics, Building 8-Room 401, NIDDK, National Institutes of Health, Bethesda, MD 20892. Tel.: 301-496-3435; Fax: 301-402-3298.

0006-3495/94/08/647/09 $2.00

defines succeeding terms in the sequence. Not every term in the sequence is detectable experimentally, but in almost every case experimentally observed conductances are terms in the sequence.

To come to this conclusion, we graphed the observed multiple conductances for 37 different channel systems as a function of apparent values of n. All of these data are presented in Fig. 1, where the horizontal axis represents consecutive values of n for a given channel system, and the vertical axis is the $\log_{10}$ of the corresponding conductance value. As summarized in Table 1, the slopes of all of these systems is 1.491 ± 0.095 (sample size = 37, SD), and closely approxi-

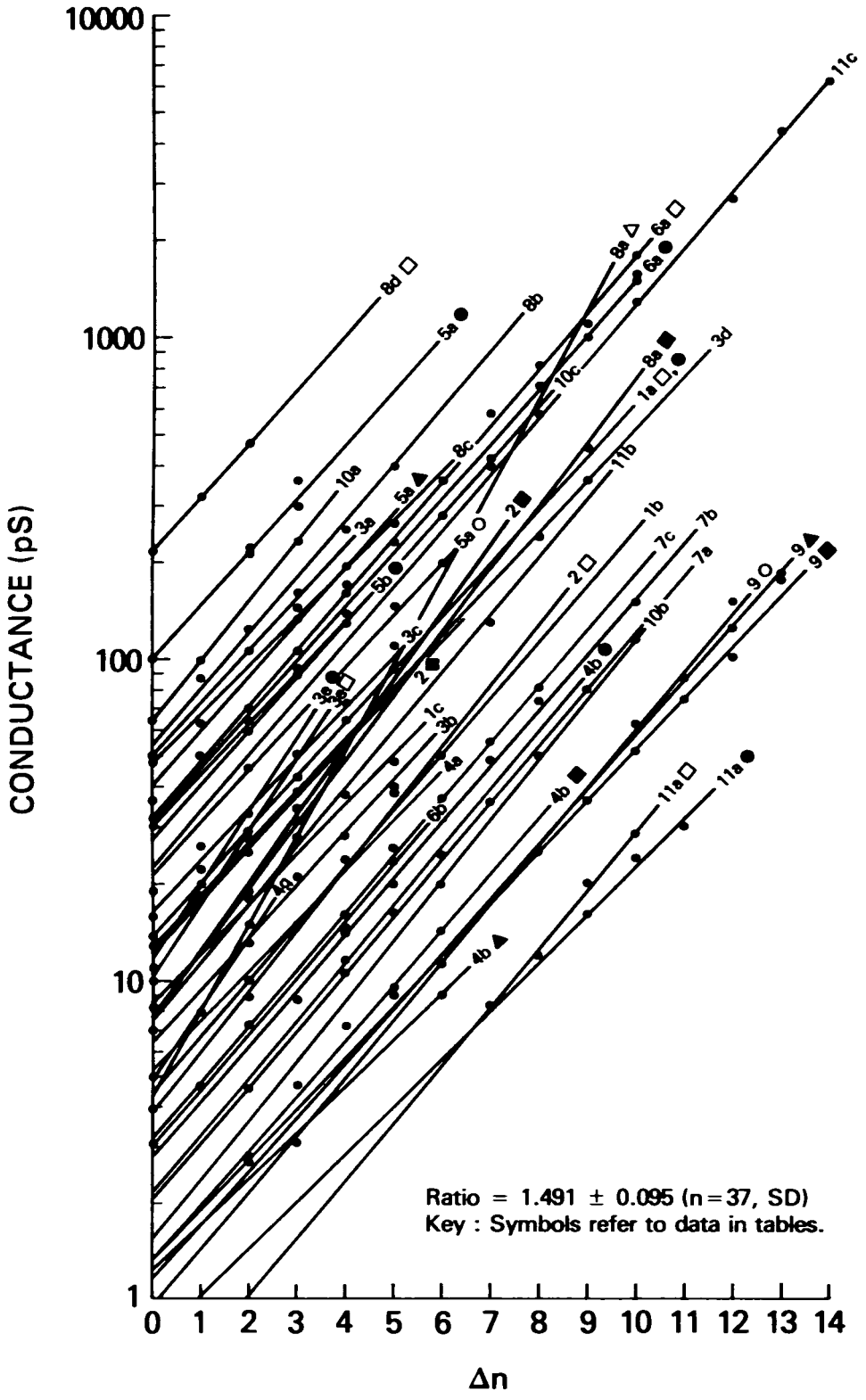

FIGURE 1 Multiple conductance levels of ion channels as a function of integer number, n. Lines are regressions of log(conductance level) vs. n, and are labeled according to descriptions in Tables 1 and 2. The horizontal axis is given as Δn because the ground state cannot be determined unambiguously.

TABLE 1 Summary of data for ion channel systems

Systemdata	Ratio*	Systemdata	Ratio
Glycine-activated Cl channel *1a*	1.463	Lobster muscle calcium release channel *6a*	1.497
GABA-activated Cl channel *1a*	1.501	Rabbit muscle L-type calcium channel *6b*	1.492
Glutamate-activated Cl channel *1b*	1.491	Human synexin calcium channel *7a*	1.557
Glutamate, aspartate, NMDA, quisqualate *1c*	1.432	Bovine lipocortin I K^+ channel *7b*	1.485
Acetylcholine, Li^+ *2*	1.516	Bovine lipocortin I K^+ channel *7c*	1.491
Acetylcholine, Cs^+ *2*	1.464	B lymphocyte anion channel *8a*	1.634
Acetylcholine, Na^+ *2*	1.566	B lymphocyte anion channel *8a*	1.828
Skeletal muscle K^+ channel *3a*	1.479	rNBF −1 (CFTR,ΔF508) chloride channel *8b*	1.509
Inward rectifier K^+ channel *3b*	1.424	Platelet chloride channel *8c*	1.421
Chromaffin granule K^+ channel *3c*	1.424	Amphibian muscle anion channel *8d*	1.464
Multi-barrel K^+ channel *3d*	1.656	Molluscan neuron chloride channel *9*	1.445
Inward rectifier K^+ channel ($+Cs^+$) *3e*	1.438	Molluscan neuron chloride channel *9*	1.481
Inward rectifier K^+ channel ($+Rb^+$) *3e*	1.438	Molluscan neuron chloride channel *9*	1.503
Heart muscle Na^+ channel *4a*	1.432	Neurohypophyseal vesicle cation channel *10a*	1.553
Heart muscle Na^+ channel (303 mM Na) *4b*	1.377	Pancreatic microsome channel *10b*	1.557
Heart muscle Na^+ channel (140 mM Na) *4b*	1.375	Gap junction channel (connexin 27) *10c*	1.430
Heart muscle Na^+ channel (70 mM Na) *4b*	1.635	Alamethicin channels (mixed) *11a*	1.344
Calcium release channel (expt. A) *5a*	1.487	Alamethicin channels (pure, KCl) *11a*	1.280
Calcium release channel (expt. C) *5a*	1.501	Alamethicin channels (mixed) *11a*	1.525
DHP-sensitive calcium channel *5b*	1.448	Alamethicin channels (pure, Tris-HEPES) *11a*	1.514
Lobster muscle calcium release channel *6a*	1.497		

* The ratio given is exp(slope of the plot of log $g_{observed}$ vs. n). The closed state ($g = 0$) is not included in the calculations. The average value is 1.491 ± 0.095 ($n = 37$, SD).

mates the ratio of ½ in the equation for the "½ Rule" given above. The specific data for each channel system is described in detail below and in Table 2, but it is immediately apparent that most of the relationships have similar slopes. This is an important conclusion, and before turning to the implications, we will first describe the data and the analysis upon which this rule is predicated.

EXPERIMENTAL DATA

The channel systems graphed in Fig. 1 and summarized in Table 1 are described in detail below. The conductance values and their assigned positions in the sequence are given in Table 2.

Excitatory and inhibitory amino acid-gated channels

Glycine and GABA-gated channels from spinal cord neurons are the principal inhibitory transmitters in the mammalian central nervous system. In cultured rat spinal cord neurons, glycine can activate a chloride channel with at least 6 conductance levels, whereas GABA can activate a different chloride channel in the same system with 5 levels of conductance (Smith et al., 1989). These data for observed values of conductance are summarized in Table 2, 1a.

Glutamate-activated channels mediate excitatory synaptic transmission in the hippocampus and other parts of the vertebrate central nervous system by action on several different receptor types. The application of glutamate to hippocampal neurons generate at least 7 discrete conductances (Jahr and Stevens, 1987). These values are shown in Table 2, 1b.

Aspartate, quisqualate, kainate, and NMDA receptors in cerebellar neurons induce multi-conductance channels with closely equivalent values for each conductance level (Cull-Candy and Usowicz, 1987). However, each ligand induced a set of conductances with distinct open probabilities, indicating that each accessed a separate system. The authors were unable to distinguish the sets of conductances *statistically* from each other, and so stated a "combined" average, which is given in Table 2, 1c.

Acetylcholine receptors

Nicotinic acetylcholine receptors (AchR) have been best studied in muscle, where multi-conductance levels occur with different frequencies. For example, although calf muscle AchRs express these subconductance states infrequently (Villarroel and Sakmann, 1992), they are extremely common in embryonic rat muscle myocytes (Hamill and Sakmann, 1981). The AchR channel is permeable to Na^+, but other cations such as Li^+ and Cs^+ also permeate the channel. As shown in Table 2, 2, each cation generates different sets of conductance levels.

Potassium channels

The calcium-activated maxi-K^+ channel from rat skeletal muscle expresses a unitary conductance in planar lipid bilayers. However, upon exposure to either dendrotoxin peptides from mamba snake venom or bovine pancreatic trypsin inhibitor, the channel exhibits multiple conductances (Lucchesi and Moczydlowski, 1991). These data are shown in Table 2, 3a.

The inwardly rectifying K^+ channel from guinae pig heart ventricle cells might be responsible for determining the resting potential across the sarcolemma, and might play a role in the repolarizing phase of the cardiac action potential. These channels can infrequently be shown to exhibit at least four conductance levels (Sakmann and Trube, 1984). In about 20% of experiments performed by a separate set of investigators (Matsuda et al., 1989), this channel can also be shown to be differentially blocked to a distinct set of 3 conductance levels by exposure to small amounts of either Cs^+ or Rb^+ (Table 2, 3e).

Chromaffin granules are secretory vesicles from the adrenal medulla (Pollard et al., 1985), the membranes of which contain a calcium-independent potassium channel (Arispe et al., 1992b). Upon reconstitution of membranes into planar lipid bilayers, five discrete conductance levels can be detected (see Table 2, 3c).

Multi-barrelled K^+ channels from the early distal tubules of the kidney of *Amphiuma* have been previously characterized in terms of a model featuring four parallel, equally conductive subunits (Hunter and Giebisch, 1987). Our own analysis of these data was complicated by the fact that not all conductances were given explicitly. Therefore, we computed possible values of conductance by taking into account the reported ohmic properties of this channel, the published record of single channel activity, and the amplitude histogram. The values are given in Table 2, 3d.

Sodium channels

Sodium channels in striated muscle are involved in propagation of the action potential from the motor end plate to the T-tubule system. In guinea pig

TABLE 2 Summary of channel systems and conductances

Channel system	$[n]g_{observed}$
Glycine and GABA-Gated chloride channels:	
1a. □ glycine	: [1]14, [2]20, [3]30, [4]43, [5]64, [6]93.
● GABA	: [1]13, [2]20, [3]29, [4]43, [5]71.
1b.	: [1]5, [2]-, [3]10, [4]15, [5]24, [6]38&40, [7]50.
1c.	: [1]8.3±0.6, [2]-, [3]18±0.5, [4]28±1.4, [5]38±0.8, [6]48±0.7.
Embryonic acetylcholine receptor channels	
2. ◆ Ca^+	: [1]11, [2]-, [3]25, [4]34.
■ Na^+	: [1]8, [2]-, [3]19, [4]31.
□ Li^+	: [1]4, [2]-, [3]9, [4]14.
Potassium channels	
3a.	: [1]50, [2]-, [3]107, [4]162.5.
3b.	: [1]7, [2]-, [3]13, [4]21, [5]28.
3c.	: [1]16, [2]26, [3]-, [4]50, [5]73, [6]95.
3d.	: [1](7.9), [2]-, [3]18.2, [4]27.7, [5]36.9.
3e. □ Ca^+	: [1]10, [2]-, [3]20, [4]30.
● Rb^+	: [1]11, [2]-, [3]22, [4]33.
Sodium channels	
4a.	: [1]5, [2]8, [3]-, [4]15.
4b. ▲ 71.5 mM	: [1](2.07), [2]3.1±0.9, [3]-, [4]9.0±1.8.
■140 mM	: [1](2.81), [2]4.7±0.6, [3](7.10), [4](9.51), [5]14.2±0.8.
● 303 mM	: [1](4.65), [2]8.7±0.3, [3](11.5), [4]16.2±1.2, [5]20.33, : [6]24.5±1.7.
Calcium release channels	
5a. ● Expt. A	: [1]100, [2]-, [3]228, [4]300 or 360.
■ Expt. B	: [1]224, [2]-, [3]440.
▲ Expt. C	: [1]36.6, [2]63.4, [3]-, [4]134, [5]192.
○ Expt. D	: [1]45.9, [2], [3]91.7, [4]147, [5]200.
□ Expt. E	: [1]92.3, [2]-,[3]173.
5b. △ Expt. B′	: [1]40, [2]73.
○ Expt. C′	: [1]98, [2]126.
● Expt. D′	: [1]30.7, [2]-, [3]64, [4]93.3.
6a. □ (i)	: [1]32, [2]50, [3]70, [4]106, [5]160&170, [6]232&264, [7]360, [8]580, [9]816, [10]1200, [11]1800.
● (ii)	: [1]30, [2]50, [3]-, [4]100, [5]-, [6]208, [7]-, [8]-, [9]712, [10]1000&1050, [11]1500&1560.
6b. ○ (i)	: [1]3.1, [2]-, [3]7.25, [4]11.3.
△ (ii)	: [1]-, [2]4.7, [3]-, [4]11.5, [5]14.6.
■ (iii)	: [1]-, [2]-, [3]-, [4], [5]15.5, [6]23.6.
Annexin calcium channels	
7a.	: [1]10.6, [2]16.5, [3]-, [4]35.75.
7b.	: [1]14, [2]20, [3]32, [4]48, [5]74, [6]96, [7]150, [8]224.
7c.	: [1]16, [2]25.7, [3]36.4, [4]54.7, [5]80.7.
Anion channels	
8a. ■ Ch1	: [1]40, [2]-, [3]-, [4]200, [5]300, [6]454.
△ Ch2	: [1]40, [2]-, [3]120, [4]-, [5]400, [6]582.
8b.	: [1]50, [2]87.5, [3]125, [4]162, [5]250, [6]450.
8c.	: [1]48, [2]-, [3]96, [4]144, [5]192.
8d. □ grad	: [1]217, [2]320, [3]465.
● sym	: [1]70, [2]-, [3]-, [4]-, [5]260.
9. ■	: [1]12.5±1.7, [2]-, [3]25±1.5, [4]36±2.5, [5]51.8±4.4, [6]74±5. [7]100±5.1, [8]177.
▲	: [1]12.5±1.7, [2]-, [3]25±1.5, [4]36±2.5, [5]62.5±3.3, [6]87.5±5 [7]126±4.8, [8]165±7.7.
○	: [1]12.5±1.7, [2]-, [3]25±1.5, [4]-, [5]62.5±3.3, [6]87.6±5, [7]150.1±6.3, [8]201±6.2.
Non-selective channels	
10a.	: [1]63, [2]98, [3]-, [4]236.
10b.	: [1]20, [2]-, [3]50, [4]80, [5]115.
10c. □ 27	: [1]140, [2]304, [3]456.
● 43	: [1]60, [2]90.
△ 32	: [1]130.
Alamethicin channels	
11a. ◆ .nS	: [1]8.46, [2]11.9, [3]15.9, [4]23.8, [5]30.
□ .nS	: [1]8.46, [2]11.9, [3]20, [4]27.6.
11b. pS	: [1]8, [2]-, [3]-, [4]-, [5]47, [6], [7]-, [8]130, [9]240, [10]360.
11c. pS	: [1]19, [2]-, [3]-, [4]-, [5]-, [6]-, [7]280, [8]-, [9]-, [10]-, [11]1300, [12]-, [13]2700, [14]4400, [15]6200.

cardiac myocytes (Nilius et al., 1989), sodium channels, for which inactivation was blocked by the Sandoz drug DPI-201-106, are reported to occur with at least three conductance levels (see Table 2, 4a). However, sodium channels from the *rat* cardiac ventricle (Schreibmayer et al., 1989) have been shown to occur in *six* conductance levels. The conductance data available for our analysis were obtained in three NaCl concentrations, and were described by the authors with two levels of certainty (Table 2, 4b).

Calcium channels

The sarcoplasmic reticulum in vertebrate skeletal muscle contains a complex that is involved in excitation-contraction coupling. The complex binds the muscle toxin ryanodine, and when incorporated into planar lipid bilayers exhibits multiple conductance levels. The variety of conductances observed with *sodium* carrying the current are summarized in Table 2, 5a (Liu et al., 1989). The data in these tables do not correspond to the stated values given explicitly by the authors, but are calculated from the calibrations provided adjacent to the records labeled A–E. In other experiments in the same paper, this channel was studied with Ca^{2+} as the charge carrier (Liu et al., 1989). Data are given in table 2, 5b, where the labels, B′-D′, correspond to similarly labeled experiments in the original paper. In this case, we also recalculated conductance data from the various conditions exactly as we did for the data in Table 2, 5a.

The calcium release channel in lobster skeletal muscle is also ryanodine-sensitive, and can be incorporated into planar lipid bilayers for analysis (Arispe et al., 1992c). With Na^+ carrying the current, a multitude of conductance levels can be observed, ranging from approximately 30–1800 pS (Table 2, 6a). With 32 pS as the preferred conductance, 11 of 17 conductances could be fit reasonably closely (Table 2, 6a [i]). However, six values could not. These included 30, 100, 208, 712, 1000 or 1050, and 1500 or 1550 pS. However, using the level of 208 pS as a *second* preferred conductance, we were able to generate a *second* set of predicted values that were well within 10% of the other 5 missing values (Table 2, 6a [ii]). From these data and the analysis, we conclude that channel heterogeneity can occur, and that in at least this one case, this heterogeneity can be completely accounted for by the ½ Rule. We will return to this hypothesis when we compare apparently impure and purified alamethicin (Table 2, 11a), and an even more complicated anion channel in a molluscan neuron (Table 2, 9).

Dihydropyridine (DHP)-sensitive, L-type calcium channels from skeletal muscle transverse tubules respond to depolarization of the muscle cell plasma membrane by allowing calcium to enter the cell. This channel has been incorporated into planar lipid bilayers (Ma and Coronado, 1988), and with Ba^{2+} as the charge carrier two sets of three conductance levels each were detected and recalculated from the slope conductances (Table 2, 6b [i and ii]). By contrast, in a study of *purified* DHP-sensitive calcium channels (Smith et al., 1987) only two conductances were reported. These were generally termed "12–14 pS" and "22 pS," which we recalculated exactly from

the published data (Table 2, 6b [iii]). The entire set of conductances can be interpreted as terms in one geometric sequence.

Annexin calcium channels

Members of the annexin gene family (Pollard et al., 1992; Raynal and Pollard, 1994), such as synexin (Annexin VII: Pollard and Rojas, 1988; Burns et al., 1990), endonexin II (Annexin V; Rojas et al., 1990), and lipocortin I (Annexin I; Pollard et al., 1992) form cationic channels across planar lipid bilayers. The channels are selective for Ca^{2+} and behave with the multi-ion calcium channel properties. Recombinant human synexin channels, reconstituted in a bilayer at the tip of a patch pipet (Burns et al., 1990) reveal three conductances calculated from records made with Ca^{2+} as the charge carrier (Table 2, 7a). Recent studies with one preparation of lipocortin I (cf. Pollard et al., 1992; N. Arispe, E. Rojas and H. P. Pollard, unpublished data) have shown that different sets of conductance levels could be detected on different days, but that both sets are internally consistent and can be predicted by the ½ Rule. On one occasion, 8 conductance levels were noted (Table 2, 7b), whereas in another series of measurements, only 5 conductances were observed (Table 2, 7c). For this well defined, pure channel protein, the "½ Rule" ratio is sustained, whereas the exact conductance values are not.

Anion channels

Anion channels of unknown function occur in B-lymphocytes and are reported to exhibit multiple conductance levels (Bosma, 1986, 1989). Our own close inspection of the data revealed a variety of conductances, in addition to some explicitly stated by the author. These are all listed in Table 2, 8a.

The cystic fibrosis transmembrane regulator (CFTR) is thought to be an anion channel, and the ΔF508 mutation in this molecule is apparently responsible for 75–80% of cases of cystic fibrosis. The recombinant NBF-1 domain has been reconstituted into planar lipid bilayers, where anion channel activity has been found to occur in multiple, interconverting conductance states (Arispe et al., 1992a). The conductances for the ΔF508 mutant NBF-1 are shown in Table 2, 8b. The wild-type protein exhibits a similar set of conductances. Furthermore, in the presence of ATP, the channel is blocked to lower conductances, including a 9-pS level, which is also predictable from the sequence.

Anion channel activity occurs in human platelets with multiple conducting levels (Mahaut-Smith, 1990). The functions are not known, but they are activated by internal calcium, and they may be involved in platelet activation and exocytotic secretion (Pollard et al., 1977). Histograms constructed from the data reveal at least four conductance levels (Table 2, 8c).

Skeletal muscle has a "high conductance, multisublevel anion channel" that might be important in setting the resting membrane potential. At least four conducting states have described the channel in adult frog muscle (Woll et al., 1987). Different sets of conductances can be detected using either symmetric or asymmetric salt concentrations on either side of the channel (Table 2, 8d).

As a final example from the class of anion channels, we have considered the system from the neurons of the fresh water mollusc, *Lymnaea stagnalis* (Getetyuk and Kazachenko, 1985). This anion channel is activated by K^+ and Ca^{2+}, and up to 16 substates have been reported. This system was once described as the "world record" for multiple conductance states in the review by Meves and Nagy (1989). We could not account for all observed conductances with one single series based on the "½ Rule". However, Getelyuk and Kazachenko had been impressed by the fact that in some experiments the activity looked "as if (there were) three independent channels with the conductances of 50, 62.5, and 87.5 pS." Indeed, expansion of each of these values by the "½ Rule" yields a complete correspondence to the entire set of observed conductances (Table 2, 9).

Other anion channels have been described that have only two levels. Such "double-barrelled" anion channels have been noted in Torpedo electroplax (Hanke and Miller, 1982; Bauer et al., 1991), rabbit cortical collecting duct (Sansom et al., 1990), and chick embryo myotubes (Schwarze and Kolb, 1984). With only two conductance states to consider, analysis by the ½ Rule seems inappropriate, and we have not included any of these data in our analysis.

Nonselective channels

Neurosecretory granules from the bovine neurohypophysis contain neurophysin and oxytosin. The granule membranes can be purified and reconstituted into tip-dip lipid bilayers, where they express both an anion channel and a nonselective, calcium-activated cation channel (Lee et al., 1992). A correlation with calcium signalling leading to exocytosis has been sought as a role for this channel. As shown in Table 2, 10a, the channel expressed at least three nonzero ohmic conductance states in symmetrical 150 mM KCl.

Microsomes from the rough endoplasmic reticulum of canine pancreas are a source of ion channel activity, which is believed to be involved in the protein synthetic process. The channel can be detected upon reconstitution of the channels into planar lipid bilayers (Simon et al., 1989), and at least four active conductance levels have been observed (Table 2, 10b).

Gap junctions are oligomeric assemblies of proteins, termed connexins 27 (kDa), 32 (kDa), and 43 (kDa), which are responsible for movement of ions and small molecules between cells (Spray and Bennett, 1985). The individual subunits also express nonselective ion channel activity when reconstituted into planar lipid bilayers (e.g., connexin 27: Young et al., 1987), or when expressed recombinantly in xenopus oocytes (e.g., connexins 32 and 43; Spray et al., 1992). From a conductance histogram, purified connexin 27 can be shown to exhibit at least three well defined open conductivity states. Recombinant connexin 43 expresses two conductance states. Connexin 32 expresses only one defined conductance of 130 pS (Table 2, 10c).

Alamethicin is a small cyclic peptide antibiotic whose structure is well known, and that forms multiple conductance, *nanoseimen* channels in planar lipid bilayers. The channels are believed to be formed by transmembrane polymers of the antibiotic, and the different conductance states have been associated with different degrees of polymerization. One of the earliest studies on a crude sample of alamethicin (Gordon and Haydon, 1972) is summarized in Table 2, 11a. In this case, only four of the seven conductances in the nS range could be assigned by the "½ Rule". Building on the experience with heterogeneity in protein channels, we soon found that the remaining three conductances could be fit by a separate "½ Rule" system. In later years, more pure preparations of alamethecin became available. Experiments with alamethecin RF30 (Hanke and Boheim, 1980) are summarized in Table 2, 11b and 11c, in which the data can be fit by single geometric sequences.

STATISTICAL VERIFICATION OF THE ½ RULE

To calculate the average value of the ratio, P, in Fig. 1, we were forced to make explicit choices regarding which conductance to assign a given value of n. In many cases, we correlated predicted values with a vacancy in the set of observed conductances to preserve the integrity of the entire sequence. In our view, such vacancies could perhaps reflect low frequency events. In any case, in general we were forced to accept the literature data at face value. However, we were concerned that in assigning values of n in this manner we were inadvertently enhancing the probability that P would have an average value of ½. From a consideration of the relationship, $g_n = g_o(P)^n$, it is possible that as P becomes small the "Rule" may begin to predict observed conductances with more accuracy. However, concommittantly, there would be an increase in the number of conductances that were terms in the sequence but not experimentally observed. In the extreme case, such a "rule" would be no rule at all.

To evaluate the statistical significance of the ½ Rule, we therefore analyzed the data from two different perspectives. One approach was to search explicitly for the assignments that yielded a minimum error with the fewest vacancies. The second was to make no assumptions and optimize the pa-

rameters by minimizing residuals using Marquardt's algorithm. As shown below, both approaches verified that a P value of ½ was quite accurate, and that the assignments shown in Fig. 1 and Table 2 were optimal.

Estimation of optimal P-value with a minimum in vacancies

Our first approach was to develop a definition for an optimal ratio (P), in which all possible assignments of n would be taken into account. According to this definition, the optimal P is the ratio that yields a minimum in error measurement while still giving a very low number of vacancies. Therefore, we let the value of P vary between 1.1 and 2.0 and correlated values of n with each of the observed and predicted conductances. Where a choice had to be made between two possibilities, we picked the one with the smallest difference. We then calculated both the root-mean-square-error (σ) between observed and predicted values of conductance and the number of vacant predicted conductances. For this analysis, we selected the 12 simple systems having more than 3 observed conductances and only zero or one vacancy according to the predictions using P = ½. For simplicity, we selected six of these systems for display. As shown in Fig. 2, a small ratio (e.g., P = 1.1 or 11/10) was very accurate but contained a large number of vacancies. As the value of the ratio rose, the value of σ also rose and then dropped to a minimum in the vicinity of 1.5 ("½"). Thereafter, the value of σ rose inexorably with an increase in P. In all cases, the number of vacancies dropped as P increased. In three cases (e.g., Fig. 2, A, D, and E), the minimum in the error coincided with zero vacancies. In one other case (Fig. 2 B), the minimum in the error at P = 1.5 corresponded to one vacancy. However, with the transition to no vacancies at P = 1.6, the error doubled. In the two remaining cases, (Fig. 2, C and F), the transitions to zero vacancies, each at P = 1.7, corresponded to minima in the error, which in both cases were substantially greater than the error at P = 1.5. It is worth noting that the slopes estimated from the plot in Fig. 1, and recorded in Table 1, correspond, as they should, to the value of P corresponding to the least error. For the simplest cases, the choice of ½ for P produces a series that successfully accounts for all of the observed conductances, yields very few vacancies, and gives a position in the error graphs at a very low minimum. For at least these cases, the assignment of n used to generate Fig. 1 is justified. It was on this basis that we tentatively extended the ½ Rule to the more complicated, heterogeneous systems.

Optimization of parameters by minimizing residuals using Marquardt's algorithm

Marquardt's algorithm (Marquardt, 1963) was used in two different calculations of the "empirical ratio" that would minimize the residual

$$r^2 = \sum_{j=1}^{N} \{g_j - G_j\}^2,$$

where g_j represents the observed and G_j the predicted conductance level. The first calculation allowed us to find the values of the parameters P_1 and P_2 used to define the general

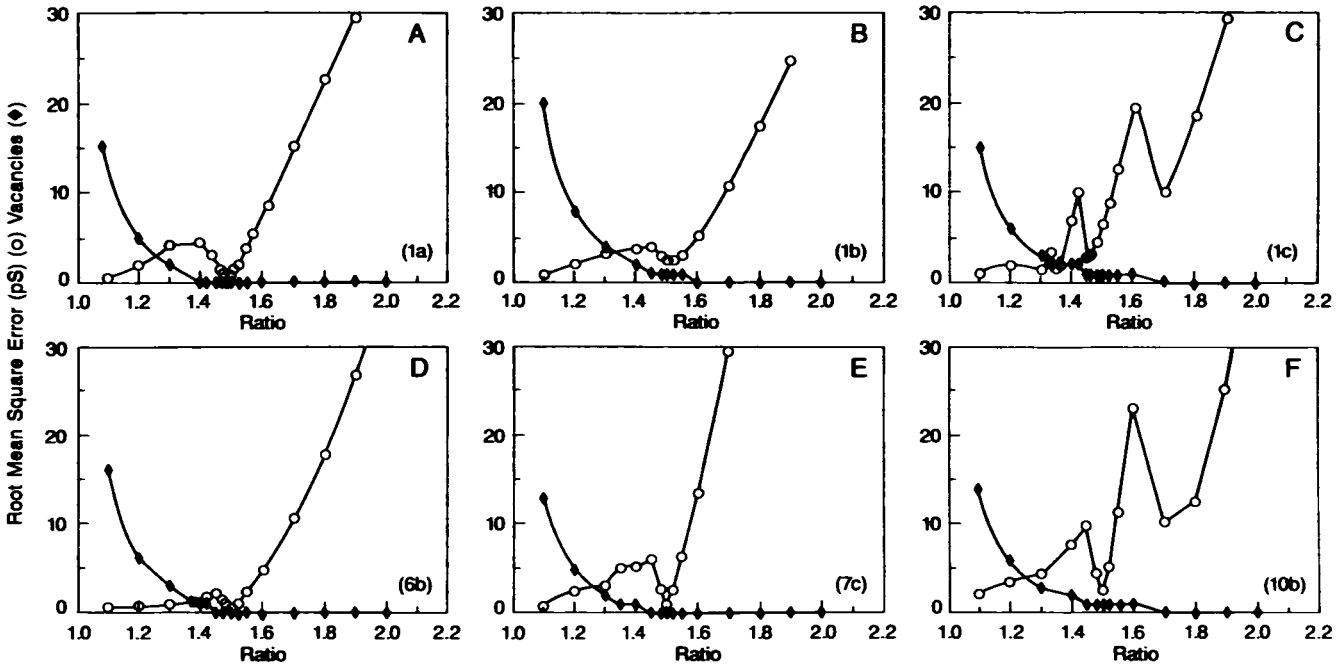

FIGURE 2 Composite graphs of root-mean-square-error (σ) and vacancies (n) for six simple channel systems. (A) Glycine-activated channel, 1a. (B) Glutamate-activated channel, 1b. (C) Excitatory amino acid channel, 1c. (D) Dihydropyridine-sensitive calcium channel, 6b. (E) Lipocortin I channel, 7c. (F) Rough endoplasmic reticulum channel, 10b. Symbols are ○ (RMS error) and ◆ (number of vacancies).

term G_j of the geometric progression, i.e.,

$$G_j = P_1\{P_2\}^j, \qquad j = 1, 2, \cdots, N.$$

To minimize the residual r^2 we used a PC Fortran version of the Marquardt's algorithm suitable for our task. The program varied each parameter at a time, and after successive iterations, generated the values of P_1 and P_2 for the best fit (see Fig. 3). The best values were $P_1 = 0.65$ and $P_2 = 1.49$ ($r^2 = 12.4$).

The first calculation required the alignment of the terms of both the theoretical geometric progression G_j along the observed conductances g_j. Obviously, the sequences started with G_1 aligned with g_1. In the majority of the cases, this alignment created "vacancies" on both observable and predicted conductance sequences. Using the arbitrary ratio of ½ in 6 out of the 28 sets representing well defined systems, no vacancies were encountered. In 17 sets, only one predicted level was vacant, and in 5 sets 2 vacancies were found. It could be argued that an arbitrary choice of the ordinal "j" for the vacant positions of measured levels g_j during the alignment of the observable and theoretical values might favor the selection of a specific ratio, i.e., ½. Therefore, we considered desirable to optimize this selection of the ordinal "j" using a statistical restraint. We noted only one vacancy at "$j = 2$" in 17 out of the 28 sets of data examined. This posed a further restriction of choice. For these sets of data pairs, the residual r^2 calculated with our choice of vacancy, i.e., "$j = 2$", was compared with the r^2 value obtained when "j" assumed values ≥ 3. A computer program prepared to achieve such a selection showed that the ordinal for the vacant g_j, which minimized r^2, was indeed "$j = 2$" in all 16 sets. For simplicity, the second calculation considered the same two free-parameters, namely P_1 and the ratio P_2, and included only 17 with only one vacancy out of the 28 sets and started the computations by arbitrarily matching the ordinal "j" representing the vacancy g_j. We next proceeded to pool all of the pairs (125 "g_j, G_j" pairs) that were arbitrarily aligned and proceeded to calculate the theoretical alignment that would minimize the residual. With fixed P_1 (=0.66) and P_2 (=½), we found 15 matches between the pairs arbitrarily aligned and the best alignment that minimize the residual ($r^2 = 10.9$). The pairs produced double occupancy of level 3. From these calculations, we concluded that, to a first approximation, for any multi-level ion channel the observable conductance levels follow a geometric sequence with a ratio P equal to ½.

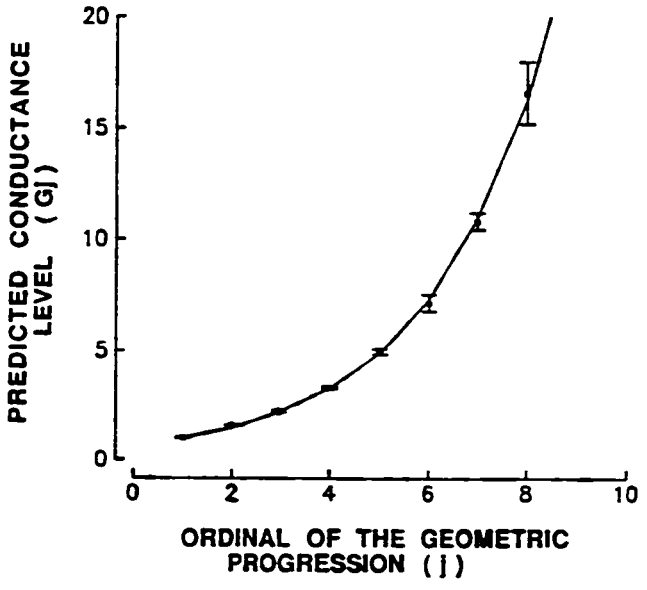

FIGURE 3 Predicted conductance levels as a function of the ordinal (j) of the geometric progression using Marquardt's algorithm. The error bars are SEM (n = 125 pairs; the regression error is 0.09). The curve is the theoretical prediction for the progression. The points are mean values of the experimental data from 1a(gly), 2(Li^+), 2(Cs^+), 2(Na^+), 3a, 3b, 3e(Cs^+), 3e(Rb^+), 3d, 4a, 5b(D'), 7a, 7b, 7c, and 10a.

CONCLUSIONS AND IMPLICATIONS

The foregoing information shows that the geometric sequence defined by $g_n = g_o(½)^n$ accurately predicts allowed multiple conductance levels of many different ion channel systems. The accuracy of the constant ratio of "½" was estimated from a plot of $\log(g_n)$ as a function of n, using the experimental conductance values from Table 2 and the corresponding values of n. We estimated the average value (sample size = 37) of the constant ratio as 1.491 ± 0.095 (mean ± SD), or 1.491 ± 0.015 (mean ± SEM). For this calculation, we omitted any data for which only two points were available (5 instances from two channel systems). The individual values are shown in Table 1. We conclude that for the purpose of describing allowed conductances, the ½ Rule is accurate to within *ca.* 1–6%. It is of course important to emphasize that we do not know whether this variance is caused by experimental error or to small but specific differences between channel systems. A composite comparison between observed and predicted conductances for all 37 channel systems is shown in Fig. 4. The slope is very close to the ideal value of unity.

As described in our introductory remarks, one conventional explanation for multiple conductance ion channels has been that each conductance level represents a different effective cross sectional area of the channel pore. This idea is based on data from alamethicin (Hanke and Boheim, 1980), and has been succinctly summarized by Stein (1990). However, the calculations underlying the model are based on the assumption that the specific conductance of the channel is that of the bulk solution. Yet, given the spatial constraints of the conducting pathway, such a premise seems especially difficult to justify (Stein, 1990). Finkelstein (1985), among others, has also made a cogent case for the ". . . (lack of a) . . . simple correlation between channel conductance and experimentally determined channel size."

Furthermore, the model based on increases in cross sectional area created by sequentially adding "barrel staves," or other units, has a more fundamental problem. It will not yield a set of areas with adjacent conductances having a constant ratio to one another as the experimental data show. Rather, this ratio will progressively *decline* towards 1.0 with increas-

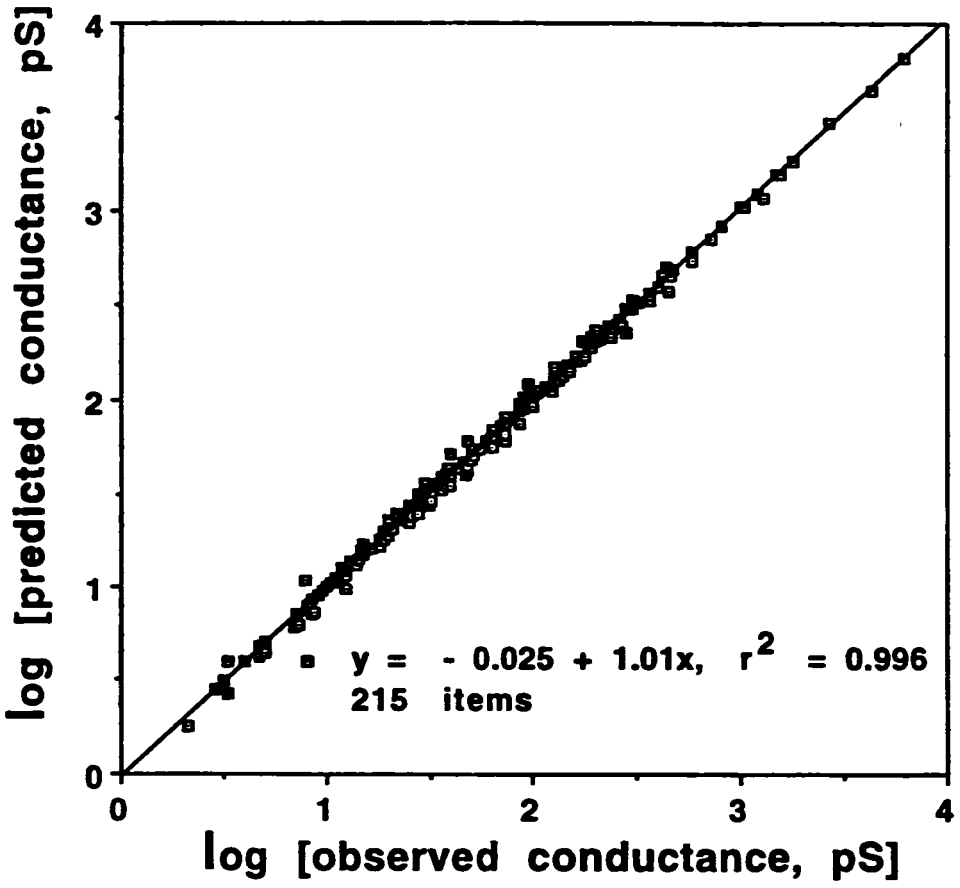

FIGURE 4 Composite ½ rule comparison of 37 channel systems from 26 different types of channels. The data from Table 2 were plotted against predicted values calculated from the ½ Rule and displayed on a log/log scale. The r^2 term is the correlation coefficient.

ing numbers of units added to the perimeter of the conducting pathway. Thus, a small increase in a large perimeter of a circle will yield an insignificant increase in the enclosed area. Thus, the "½ Rule" and the barrel stave model are mathematically exclusive. A similar, progressive *decline* also occurs for ratios of terms in different binomial distributions. We have concluded, therefore, that the parallels between the alamethicin channels and other protein-based channels, both membrane resident and reconstituted, indicate that the biophysical basis of the "½ Rule" might lie outside the requirements of any specific channel system and, rather, have something to do with the fundamental properties of the pore in ion channels.

We conclude finally with the observation that although we cannot assign an unambiguous structural interpretation to the ½ Rule, this does not obviate the utility of the relationship for accurately describing allowed conductance states of a wide variety of ionic channels. The advantage of this rule is that it is both relatively accurate and inclusive for the 26 types of channels studied. Furthermore, the rule provides a descriptive framework for other experimentally determined channel properties, including channel heterogeneity, effects of channel blocking ions and ligands, and experimental variation in specific channel conductance on different days and in different laboratories. The fact that the ½ Rule is a power function also hints at a common energetic basis for the relationship. For example, a ratio of ½ between different conductances corresponds to an energy barrier of 0.24 kcal/mol. Finally, it is our expectation that further studies of multiple conductance levels in ion channels, particularly with respect to a search for deviations from the ½ Rule, might eventually lead to a more complete understanding of ion channel function.

The authors thank to Drs. Ofer Eidelman, Enrique Jaimovich, Allen P. Minton, Adrian Parsegian, John Rinzel, Wilfred Stein, and Gal Yadid for their valuable comments to the work while it was in progress, and to Mr. Rodrigo Jaimovich for his contribution to graphical analysis.

REFERENCES

Arispe, N., E. Rojas, J. Hartman, E. Sorscher, and H. B. Pollard. 1992a. Intrinsic anion channel activity of the wild type and the Δ F 508 forms of the recombinant first nucleotide binding fold domain of the cystic fibrosis transmembrane regulator protein. *Proc. Natl. Acad. Sci. USA.* 89:1539–1543.

Arispe, N., E. Rojas, and H. B. Pollard. 1992b. Calcium independent potassium channels in chromaffin granule membranes. *J. Membr. Biol.* 30: 191–202.

Arispe, N., E. Olivares, E. Jaimovich, and E. Rojas. 1992c. Reconstitution of ryanodine receptor calcium channels from lobster muscle sarcoplasmic reticulum in planar lipid bilayers. *Biophys. J.* 61:24*a*. (Abstr.)

Bauer, C. K., K. Steinmeyer, J. R. Schwarz, and T. J. Jentsch. 1991. Completely functional double-barreled chloride channel expressed from a single Torpedo cDNA. *Proc. Natl. Acad. Sci. USA.* 88:11052–11056.

Baumann, G., and P. Mueller. 1974. A molecular model of membrane excitability. *J. Supramol. Struct.* 2:538–557.

Bosma, M. M. 1986. Ph.D. Thesis, Department of Physiology, UCLA (Quoted in Fox, 1987).

Bosma, M. M. 1989. Anion channels with multiple conductance levels in a mouse B lymphocyte cell line. *J. Physiol.* 410:67–90.

Cull-Candy, S. G., and M. M. Usowicz. 1987. Multiple-conductance channels activated by excitatory amino acids in cerebellar neurons. *Nature.* 325:525–528.

Edwards, C. 1982. The selectivity of ion channels in nerve and muscle. *Neuroscience.* 7:1335–1366.

Finkelstein, A. 1985. The ubiquitous presence of channels with wide lumens and their gating by voltage. *Ann. N.Y. Acad. Sci.* 456:26–32.

Fox, J. A. 1987. Ion channel subconductance states. *J. Membr. Biol.* 97:1–8.

Geletyuk, V. I., and V. N. Kazachenko. 1985. Single channels in molluscan neurons: multiplicity of the conductance states. *J. Membr. Biol.* 86:9–15.

Gordon, L. G. M., and D. A. Haydon. 1972. The unit conductance channel of alamethicin. *Biochim. Biophys. Acta.* 255:1014–1018.

Hamill, O. P., and B. Sakmann. 1981. Multiple conductance states of single acetylcholine receptor channels in embryonic muscle cells. *Nature.* 294: 462–464.

Hanke, W., and G. Boheim. 1980. The lowest conductance state of the alamethicin pore. *Biochim. Biophys. Acta.* 596:456–462.

Hanke, W., and C. Miller. 1982. Single chloride channels from *Torpedo* electroplax. Activation by protons. *J. Gen. Physiol.* 82:25–45.

Hille, B. 1984. Ionic Channels of Excitable Membranes. Sinauer Associates, Sunderland, MA. 426 pp.

Hunter, M., and G. Giebisch. 1987. Multi-barelled K channels in renal tubules. *Nature.* 327:522–524.

Jahr, C. E., and C. F. Stevens. 1987. Glutamate activates multiple single channel conductances in hippocampal neurons. *Nature.* 325:522–525.

Latorre, R., and O. Alvarez. 1981. Voltage-dependent channels in planar lipid bilayers. *Physiol. Rev.* 61:77–150.

Lucchesi, K. J., and E. Moczydlowski. 1991. On the interaction of bovine pancreatic trypsin inhibitor with maxi Ca^{2+}-activated K^+ channels. A model system for analysis of peptide-induced subconductance states. *J. Gen. Physiol.* 97:1312–1319.

Lee, C., G. Dayanithi, J. J. Nordmann, and J. R. Lemos. 1992. Possible role during exocytosis of a Ca^{2+}-activated channel in neurohypophysial granules. *Neuron.* 8:335–342.

Liu, Q.-Y., F. A. Lai, E. Rousseau, R. V. Jones, and G. Meissner. 1989. Multiple conductance states of the purified calcium release channel complex from skeletal sarcoplasmic reticulum. *Biophys. J.* 55:415–424.

Ma, J., and R. Coronado. 1988. Heterogeneity of conductive states in calcium channels of skeletal muscle. *Biophys. J.* 53:387–395.

Mahaut-Smith, M. P. 1990. Chloride channels in human platelets: evidence for activation of internal calcium. *J. Membr. Biol.* 118:69–75.

Marquardt, D. W. 1963. An algorithm for least-squares estimation of nonlinear parameters. *J. Soc. Ind. Appl. Math.* 11:431–441.

Matsuda, H., H. Matsuura, and A. Noma. 1989. Triple-barrel structure of inwardly rectifying K^+ channels revealed by Cs^+ and Rb^+ block in guinae-pig heart cells. *J. Physiol.* 413:139–157.

Meves, H., and K. Nagy. 1989. Multiple conductance states of the sodium channel and of other ion channels. *Biochim. Biophys. Acta.* 988:99–105.

Miller, C. 1982. Open-state substructure of single chloride channels from *Torpedo* electroplax. *Phil. Trans. R. Soc. B. Biol. Sci.* 299:401–411.

Nilius, B., J. Vereecke, and E. Carmeliet. 1989. Different conductance states of the bursting sodium channel in guinae pig ventricular myocytes. *Pflügers Arch.* 413:242–248.

Pollard, H. B., K. M. Tack-Goldman, C. P. Pazoles, C. E. Creutz, and N. R. Shulman. 1977. Evidence for control of serotonin secretion from human platelets by hydroxyl ion transport and osmotic lysis. *Proc. Natl. Acad. Sci. USA.* 74:5295–5299.

Pollard, H. B., R. Ornberg, M. Levine, E. Heldman, K. Morita, K. Kelner, P. Lelkes, K. Brocklehurst, E. Forsberg, L. Duong, R. Levine, and M. B. H. Youdim. 1985. Hormone packaging and secretion by exocytosis: a view from the chromaffin cell. *Vitamins and Hormones.* 42:109–196.

Pollard H. B., and E. Rojas. 1988. Calcium-activated synexin forms highly selective, voltage-gated calcium channels in phosphatidylserine bilayer membranes, *Proc. Natl. Acad. Sci. USA.* 85:2974–2978.

Pollard, H. B., A. L. Burns, and E. Rojas. 1990. Synexin: a cystosolic calcium binding protein which promotes membrane fusion and forms calcium channels in artificial bilayer and natural membranes. *J. Membr. Biol.* 117:101–112.

Pollard H. B., H. R. Guy, N. Arispe, M. de la Fuente, G. Lee, E. M. Rojas, J. R. Pollard, M. Srivastava, Z.-Y. Zhang-Keck, N. Merezhinskaya, H. Caohuy, A. L. Burns, and E. Rojas. 1992. Calcium channel and membrane fusion properties of synexin and other members of the annexin gene family. *Biophys. J.* 62:19–22.

Raynal P., and H. B. Pollard. 1994. Annexins: the problem of assessing the biological role for a gene family of multifunctional calcium-and phospholipid-binding proteins. *Biochem. Biophys. Acta.* 1197:63–93.

Rojas E., H. B. Pollard, H. T. Haigler, C. Parra, and A. L. Burns. 1990. Calcium-activated endonexin II forms calcium channels across acidic phospholipid bilayer membranes. *J. Biol. Chem.* 265:21207–21215.

Sakmann, B., and G. Trube. 1984. Conductance properties of single inwardly rectifying potassium channels in ventricular cells from guinae-pig heart. *J. Physiol.* 347:641–657.

Sansom, S. C., B.-Q. La, and S. L. Carosi. 1990. Double-barreled chloride channels of collecting duct basolateral membrane. *Am. J. Physiol.* 259: F46-F52.

Schwarze, W., and H.-A. Kolb. 1984. Voltage-dependent kinetics of an anionic channel of large unit conductance in macrophages and myotube membranes. *Pflügers Arch.* 402:281–291.

Schreibmeyer, W., H. A. Tritthart, and H. Schindler. 1989. The cardiac sodium channel shows a regular substate pattern indicating synchronized activity of several ion pathways instead of one. *Biochim. Biophys. Acta.* 986:172–186.

Simon, S. M., G. Blobel, and J. Zimmerberg. 1989. Large aqueous channels in membrane vesicles derived from the rough endoplasmic reticulum of canine pancreas or the plasma membrane of *Escherichia coli*. *Proc. Natl. Acad. Sci. USA.* 86:6176–6180.

Smith, S. M., R. Zorec, and R. N. McBurney. 1989. Conductance states activated by glycine and GABA in rat cultured spinal neurons. *J. Membr. Biol.* 108:45–52.

Spray, D. C., and M. V. L. Bennett. 1985. Gap Junctions. Cold Spring Harbor Laboratory, Cold Spring Harbor, NY. 1–409.

Spray, D. C., A. P. Moreno, B. Eghbali, M. Chanson, and G. I. Fishman. 1992. Gating of gap-junction channels as revealed in cells stably transfected with wild type and mutant connexin cDNAs. *Biophys. J.* 62:53–55.

Stein, W. D. 1986. Transport and Diffusion Across Cell Membranes. Academic Press, Orlando, FL.

Stein, W. D. 1990. Channels, Carriers and Pumps: An Introduction. Academic Press, Orlando, FL.

Woll, K. H., M. D. Leibowitz, B. Neumcke, and B. Hille. 1987. A high conductance anion channel in adult amphibian skeletal muscle. *Pflügers Arch.* 410:632–640.

Young, J. D.-E., Z. A. Cohn, and N. B. Gilula. 1987. Functional assembly of gap junction conductance in lipid bilayers: demonstration that the major 27 kd protein forms the junctional channel. *Cell.* 48:733–743.